International Journal on Emerging Technologies **10**(4): 385-394(2019)

ISSN No. (Print): 0975-8364
ISSN No. (Online): 2249-3255

Selection and Preparation of Suitable Composite Phase Change Material for PV Module Cooling

V. Karthikeyan[1,3], P. Prasannaa[2], N. Sathishkumar[3], Kanchanok Emsaeng[4], Sukruedee Sukchai[1] and Chatchai Sirisamphanwong[5]

[1]School of Renewable Energy and Smart Grid Technology, Naresuan University, Thailand.
[2]Department of Mechanical Engineering, Annamalai University, India.
[3]MinVayu, Center for Scientific Research (CSR), Windara farm, Auroville, India.
[4]Faculty of Education, Pibulsongkram Rajabhat University, Thailand.
[5]Smart Energy System Integration Research Unit, Department of Physics, Faculty of Science, Naresuan University, Thailand.

(Corresponding author: Sukruedee Sukchai)
(Received 18 September 2019, Revised 11 November 2019, Accepted 19 November 2019)
(Published by Research Trend, Website: www.researchtrend.net)

ABSTRACT: Phase Change Material (PCM) is an effective thermal energy storage material with the activation of latent heat capacity even though its low thermal conductivity creates the thermal conduction resistance during charging and discharging. Many types of research had been conducted to increase pure PCM thermal conductivity (KpPCM) by adding thermal additives. The main objective of this research is to find a suitable technique to increase the KpPCM for PV module temperature (T_{PV}) reduction. Paraffin wax is widely performed with metal and non-metal thermal additives because of its attractive thermophysical property. Metal-based composite PCM increased the KpPCM effectively but the total weight of the system increased due to the highest mass fraction of the metal additives because an increase in the total weight of the system could lead to damage to the PV module. Considering this weight effect, expandable graphite (EG) is selected as a non-metal additive that is suitable for T_{PV} reduction in terms of an effective thermal additive enhancer with less mass fraction. In this experiment, compressed EG is impregnated with liquid PCM, after impregnation again it is compressed into three different densities to find the relationship of the thermal conductivity enhancement. Composite PCM (cPCM) has undergone thermal conductivity measurement using hot-wire technology and resulting show that an increase in density of cPCM leads to enhance thermal conductivity maximum of 5.68 W/m.K for 0.79 g/cm^3.

Keywords: Thermal additives, metal foam, porous graphite foam, PCM impregnation, composite PCM, thermal conductivity enhancement.

I. INTRODUCTION

Solar energy is a well-known profitable renewable energy source among others in terms of techno-economic aspects and maintenance costs [1, 2]. PCM's are widely used for low and medium temperature applications, especially for solar thermal applications to store the thermal energy for off-sunshine hours [3]. Substantially, PCM stores thermal energy in the form of latent heat by changing its phase, without raising its own temperature than sensible heat storage materials [4]. Generally, for T_{PV} reduction it is necessary to select the appropriate PCM and thermal absorbing material unless reduction may achieve poorly [5]. However, PCM is a low thermal conducting material, eventually increasing PCM thickness leads to creating the thermal conduction resistance. Specifically, for T_{PV} reduction it is necessary to keep in mind that PCM should store the thermal energy effectively without any thermal barrier.

Many types of research had been performed to reduce the PV module temperature using pure PCM, Mahamudul *et al.*, [6, 7] poured liquid PCM on the back surface of the PV module and it leads to regulate the T_{PV} maximum of four hours when the thickness of PCM is less, PCM turns to be liquid in short period and it lost its latent heat capacity. On the other hand, an increase in PCM thickness leads to an increase in the total thermal absorbing capability [8]. But this increase in thickness leads to create the thermal conduction resistance within the PCM and it causes nonlinear T_{PV} reduction than lower thicknesses [9]. To overcome this conduction resistance, many types of research had been performed with thermal distribution heatsink. PV module back surface temperature is transferred to the PCM container with the help of thermal distribution fin which is placed on the top surface of the PCM container.

Biwole *et al.*, [10] performed CFD simulation for the system parameters of Huang *et al.*, [11] using thermal distribution fin, resulting in T_{PV} maintained less than 50℃ for 89 min and using Navier stroke equation 2D finite element model solved [12]. Some other researches are performed with different specifications of thermal distribution fin to analyze the thermal behavior such as different length [13], thickness [14] and spacing between each fin [15, 16]. Comparatively, this technique reduces the T_{PV} better than pPCM.

And later different inclination using thermal distribution fin is performed from 0° to 90° inclination [17] it was observed that 100th minute the clear variation of thermal distribution in PCM container. However thermal energy distribution occurs only around the fins and reportedly total weight of the system is high and also difficult in construction. Further considering these difficulties, available K_{pPCM} enhancing techniques are categorized in the following section to find the appropriate method.

II. METAL-BASED COMPOSITE PCM

Metal foams are often called open-cell foams which are widely used for thermal conductivity enhancement. Generally, open-cell foams are made up of high thermal conducting metal such as copper, aluminum, nickel, iron and stainless steel which are readily available in the commercial market. Metal foams are widely categorized with their physical structure such as cell type, shape, porosity, pore density or Pore Per Inch (PPI).

A. Metal foam impregnation process

The metal foam is impregnated into liquid PCM using a vacuum pump to fill the liquid PCM into the pores of metal foam as shown in Fig. 1. Poor impregnation causes empty or not fully filled pores in the foam which leads to reduce thermal conductivity because the impregnation ratio is directly proportional to the thermal conductivity enhancement. The impregnation ratio is defined by the ratio of actual mass and ideal mass which has been calculated using dimensionless Eqn. (1) [18].

$$\alpha = \frac{m_{actual}}{m_{ideal}} = \frac{\Delta m_i}{\varepsilon_b V_t \rho_{PCM}} \quad (1)$$

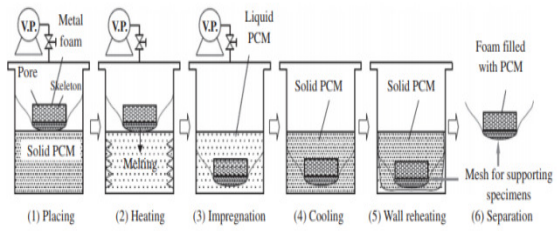

Fig. 1. Metal foam impregnation process [18].

Simulation performed to analyze thermal conductivity enhancement profile for five different metal foam (Al, Cu, Ni, SS, and polyurethane) along with three different porosity ranges (0.874, 0.942, 0.891) as shown in Fig. 2. Metal foam with 0.874 porosity enhanced maximum of 11.56 ±1.82 W/m.K for aluminum foam, 19.32±3.08 W/m.K for copper foam, 0.97±0.11 W/m.K for stainless steel foam and 4.60 ±0.69 W/m.K for nickel foam. Comparatively higher porosity leads to impregnate higher mass ratio because of its pore size and it causes to lower thermal conductivity. And 0.891 porosity foam enhanced 3.46±0.97 W/m.K for aluminum foam, 5.64±1.64 W/m.K for copper foam because a solid fraction of this porosity is lower than 0.874 porosity. Reportedly polyurethane foam thermal conductivity enhancement is not effective as compared to other metal foam due to its low thermal conductivity [19].

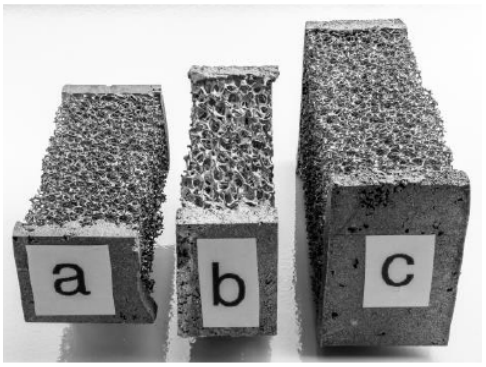

Fig. 2. Metal foam (a) Porosity=0.874, Solid fraction= 12.6%, (b) Porosity=0.942, Solid fraction= 5.8%, (c) Porosity=0.891, Solid fraction= 10.9% [19].

Xiao *et al.,* (2014) [20] investigated different pore per inch (PPI) of copper and nickel foam using paraffin wax as shown in Fig. 3. In this study, a maximum of 95% PCM impregnation is achieved using a vacuum pump and non-vacuum achieved 90 % because some pores are closed during the impregnation process [18]. Copper foam-based PCM enhanced a maximum of 16.01 W/m.K from 0.354 W/m.K and this foam increased the melting temperature of the PCM by 0.4℃ than pure PCM. And nickel foam-based PCM enhanced a maximum of 2.33 W/m.K with a 0.55℃ melting temperature increment.

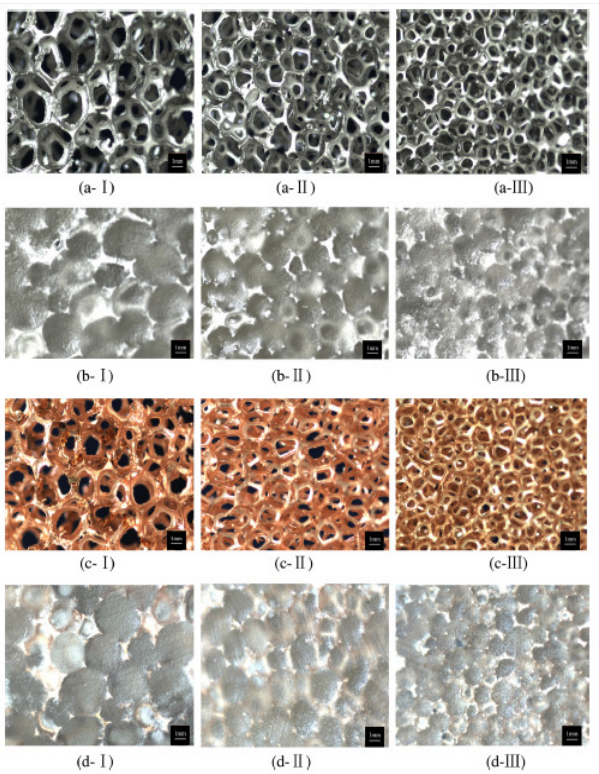

Fig. 3. (a) Nickel foam, (b) Nickel foam impregnated with PCM, (c) Copper foam, (d) Copper foam impregnated with PCM; I= 5 PPI, II= 10 PPI, III= 25 PPI [20].

Wang *et al.*, [21] conducted research on aluminum foam by impregnating them with air, water, and paraffin wax. Earlier it was stated that higher porosity cause to lower the thermal conductivity. In this research different porosity ranges are performed to optimize the appropriate range from 0.812 to 0.975. Air impregnated aluminum foam enhanced thermal conductivity from 19.56 to 1.902 W/m.K corresponding to the porosity range, water impregnated aluminum foam enhanced from 20.21 to 2.50 W/m.K to the corresponding porosity. Comparatively, water impregnated aluminum foam enhanced higher than air because water density is higher than air as well as water thermal conductivity is high. PCM impregnated aluminum foam enhanced ~12.5 to ~2.5 W/m.K to the corresponding porosity. However, this thermal conductivity enhancement is lower than water and air because of its phase-change property and lower specific heat capacity leads to restricting the thermal energy transfer into the PCM during solid-state.

In most cases, Al and Cu foam are widely investigated with PCM because of its attractive thermal conductivity with a maximum of 24.56 W/m.K. Nickel foam also examined but resulting lesser enhancement than Al and Cu foam. Further metal foam based composite PCM's are listed in Table 1 with their physical structure and corresponding to their porosity and mass fraction.

Theoretical calculation of thermal conductivity enhancement had been calculated for various porosity levels for ERG materials and aerospace [22] method as expressed in Eqn. (2).

$$K_{cPCM} = \frac{1-\varepsilon_{foam}}{3} K_{foam} \quad (2)$$

K. Boomsma method to calculate the PCM thermal conductivity using metal foamis expressed in Eqn. (3) [23].

$$K_{cPCM} = \frac{\sqrt{2}}{2(R_A + R_B + R_C + R_D)} \quad (3)$$

where,

$$R_A = \frac{4d}{\left(2e^2 + \pi d(1-e)\right)K_s + \left(4 - 2e^2 - \pi d(1-e)\right)K_f}$$

$$R_B = \frac{(e-2d)^2}{(e-2d)e^2 K_s + \left(2e - 4d - (e-2d)e^2\right)K_f}$$

$$R_C = \frac{\left(\sqrt{2} - 2e\right)^2}{2\pi d^2\left(1 - 2e\sqrt{2}\right)K_s + 2\left(\sqrt{2} - 2e - \pi d^2\left(1 - 2e\sqrt{2}\right)\right)K_f}$$

$$R_D = \frac{\sqrt{2}}{2(R_A + R_B + R_C + R_D)}$$

Table 1: List of cPCM prepared using metal additives.

PCM type	K_{pPCM}	Additive	Additive detail	K_{cPCM} (W/m.K)	Reference
Paraffin wax	0.2	Foam SS, Ni, Al, Cu	ε=0.874, f=12.6 wt%	0.97, 4.60, 11.56, 19.32	[19]
		Foam Al, Cu, SS, Ni	ε=0.942, f=5.8 wt%	3.46, 5.64, SS and Ni is less than Al and Cu	
Paraffin wax	0.354	Foam Cu and Ni	ε=0.9754,25 PPI	5.04, 1.24	[20]
			ε=0.9424, 25 PPI	11.33, 1.70	
			ε=0.9061, 25 PPI	16.01, 2.33	
Paraffin wax	–	Foam Al	ε=0.94, 10 PPI	3.67	[24]
Air		Foam Al	ε=0.812 to 0.975	19.56 to 1.902	[21]
Water	0.8	Foam Al	ε=0.812 to 0.975	20.21 to 2.50	[21]
Paraffin wax (10, 20, 30, 40 PPI gives nearly same K_{eff})		Foam Al	ε=0.812 to 0.975	~12.5 to ~2.5	[21]
		Foam Ni	ε =0.812 to 0.975	~5.5 to ~1.5	
		Foam Cu	ε =0.812 to 0.975	~24.5 to ~3.5	
Paraffin wax	0.55	Foam Al	ε =0.8, 20 PPI	12.6	[25]
$NaCO_3$	0.83	Foam Al	ε =0.8, 20 PPI	13.1	[25]
PCM		Foam Cu	f=38.5 to 46.6 wt%, PPI=40, 70, 90	0.47 at 40 PPI	[26]
		Foam Ni	f=18.5 to 22.4 wt%, PPI=40, 70, 90	1.452 at 40 PPI	
RT 42		Graphite porous matrix	ρ_{foam}=210kg/m^3 ρ_{CPCM}=789kg/m^3	16.6	[27]
Paraffin wax		Porous graphite foam	Diameter=1-3mm, ρ_{foam}=0.25 g/cm^3 ρ_{CPCM}=0.95 g/cm^3,	4.98	[28]
Paraffin wax	0.042	Foam Cu	Pore size= 2-3 mm ε =0.973, 8-12 PPI	3.112	[29]
SAT+ CMC 0.5 wt% +DHPD 2 wt% (CMC and DHPD is used to control the super cooling effect of SAT		Foam Cu	ε =0.924 to 0.973, PPI=5-25, (foam dimension 4mm*40mm*10mm)	6.8 to 3.3	[30]
Paraffin wax	0.2	Foam Al	ρ_{CPCM}=950.98 kg/m^3	2.257	[31]

III. NON-METAL BASED COMPOSITE PCM

Other than metal additives, there are many methods to increase the K_{pPCM} but this method needs special preparation for each and every non-metal additive. Comparatively, this method is more feasible in terms of easy installation with the existing system. Because metal additives are not easy to get the expected dimensions especially when the storage system or tank comes in cylindrical shape it is complicated. When it comes to non-metal additives, it can be easily composite with PCM and it can be kept in any desired dimension.

A. Graphene-based composite PCM

Nitrogen-doped graphene (NDG): Palmitic acid (PA) composited with NDG with the preparation of 1-5 wt % (Fig. 4) at 130℃ to evaporate the C_7H_8 and then prepared composite PCM is examined for 1000 thermal cycle to find thermal degradation range. Resulting shows that NDG composited PCM thermal property degradation is negligible after 1000 cycles with satisfying 4.3 J/g latent heat of fusion loss was noticed and there was no phase segregation and single-phase transition curve achieved. Thermal conductivity enhancement is not effective like metal foam but it enhanced to a maximum of 1.73 W/m.K for 5 wt %, and leakage is prevented for 3-5 wt % composition [32].

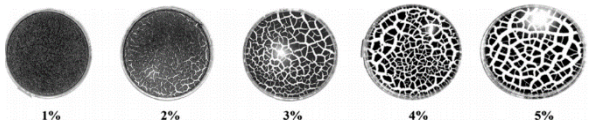

Fig. 4. Different composition rate of NDG with PA [32].

Few layer graphene (FLG): Goli *et al.,* [33], FLG composited with paraffin wax (0.25 W/m.K) at three different types of loading. Type A, FLG was loaded in the fraction of 0.5 wt % and 1 wt % with the average thickness of 0.35 nm, lateral size is between 150 and 3000 nm, and average size is 550 nm. in type B, loading factor was 20 wt % with the thickness of ~1 nm and average lateral diameter ~ 10µm, and finally type C, loading factor was 20 wt % with the average thickness of 8 nm, lateral size between 150 and 3000 nm, and average size was ~550 nm. To find the appropriate composite PCM, FLG was prepared at different dimensions and resulting shows that thermal conductivity of Type A (0.5 wt %) enhanced maximum of ~10 W/m.K, and for 1 wt % enhanced ~15 W/m.K. Type B and C enhanced maximum of ~45 W/m.K because higher mass fraction of FLG increases thermal conductivity and noticeably it is higher enhancement than metal-based composite PCM. Comparatively, multilayer graphene nanocomposite enhanced a maximum of 14 W/m.K for 2 % of volume [34].

B. Nano-PCM

Graphene nano PCM (GNP) composited with beeswax with the different mass fraction of 0.05 wt %, 0.1 wt %, 0.15 wt %, 0.2 wt %, 0.25 wt % and 0.3 wt %. Generally doping other materials with PCM leads to reduce latent heat of fusion but graphene doping was actually increased from 141.49 J/g to 186.74 J/g corresponding to the prepared mass fraction. This composition leads to an increase in thermal conductivity from 1.1 W/m.K to 2.89 W/m.K respectively [35].

Inorganic eutectic ternary carbonate salt was prepared with the combination of 33.2 wt % Li_2CO_3, 33.3 wt % Na_2CO_3 and 34.5 wt % K_2CO_3. Prepared pure ternary carbonate salt thermal conductivity was 1.32 W/m.K further to increase this eutectic thermal conductivity, Magnesium (Mg) is mixed as nanoparticle with the eutectic mixture in the form of 0.2 wt %, 0.5 wt %, 1 wt % and 2 wt% as shown in Fig. 5. Reportedly, there is a minor melting temperature variation with 2 wt % of Mg and thermal conductivity enhanced from 1.59 W/m.K to 1.93 W/m.K [36]. Noticeably Mg thermal conductivity is not high like graphene.

Fig. 5. Inorganic eutectic ternary carbonate salt with different composition of Mg [36].

C. Ultrathin-Graphite Foam (UGF)

Ji *et al.,* [37] studied the combination of UGF with paraffin wax using a hydrophobic method. Examined UGF pore diameter is 500 µm which is immersed with paraffin and consequently, 30 thermal heating and cooling cycle was conducted to measure the PCM degradation property and reportedly less than 2 % of latent heat of fusion lost after 30th thermal cycling. This degradation is negotiable in terms of enhanced thermal conductivity with the loading factor of UGF 1.23 vol. % tends to enhance the thermal conductivity by18 times (~3.5 W/m.K) and noticeably UGF pore size is less which leads to enhance better thermal conductivity. Another research, used 7 wt % xGnP which enhanced the thermal conductivity maximum of 0.8 W/m.K [38]. Short multi-walled Carbon Nano Tube enhanced maximum of 0.324 W/m.K from 0.263 W/m.K with the loading factor of 5 wt % and also reportedly high thermal conductivity enhancement achieved with graphene nano pellets was 0.7 W/m.K with 5 wt % [39].

D. Multi-layer graphite nano pellets

Adipic acid (AA) and sebacic acid (SA) eutectic mixture were prepared in the combination of 48 wt % and 52 wt %. Prepared eutectic was composited with Multi-layer graphite nanoplates (GNP) with a thickness of 5-8 nm, the surface area is 120-150 m^2/g and particle size is 5 µm. GNP composited in the range of 0.1 wt %, 0.3 wt % and 0.5 wt %.

It was known that eutectic mixtures are always good thermal energy storage materials in terms of no super cooling effect, a single transition curve with a sharp melting range. so further thermal conductivity enhancement was measured and resulting shows that less variation in enhancement due to its multi-layer such as 0.117 W/m.K, 0.122 W/m.K, and 0.131 W/m.K, respectively [46].

E. EG based composite PCM

EG is flake graphite which expands the volume of about 200-300 times at 300 – 1100 ℃ depending upon the material grades. During volume expansion, expandable graphite is becoming highly porous material. Sarı and Karaipekli [41] EG composited with paraffin wax in the form of 2, 4, 7 and 10 wt %. In this study, EG was impregnated with the liquid paraffin wax for absorption and it dried naturally. Resulting shows that the maximum of 0.4 w/m.K to 0.82 W/m.K was enhanced corresponding to their composition. And palmitic acid (PA) composited with EG using a vacuum impregnation method for proper impregnation. In this study also enhancement is not high because EG is directly impregnated with PCM which leads to absorb high PCM in it due to its high pores. In addition, cPCM was undergone for 3000 thermal cyclings, reportedly there is no material degradation was noticed [42].

Table 2: List of cPCM prepared using non-metal additives.

PCM type	K_{pPCM}(W/m.K)	Additive	Additive detail	K_{cPCM} (W/m.K)	Reference
Paraffin wax	0.263	UGF	Pore diameter=500µm f= 2 vol%	~3.5	[37]
Erythritol	0.73	CF	HP (12, 16.2 and 20.4 vol%)	~28	[40]
			MD (0.59 to 0.71 packing factor)	~4	
Paraffin wax	0.22	EG	f=2, 4, 7, 10 wt%	0.4, 0.52, 0.68, 0.82	[41]
Palmitic acid	0.17	EG	f=5, 10, 15, 20 wt%	0.2, 0.3, 0.38, 0.60	[42]
Stearic acid	0.3	EG	f=2, 4, 7, 10 wt%	0.38, 0.47, 0.84, 1.14	[43]
		CF	f=2, 4, 7, 10 wt%	0.37, 0.62, 0.79, 0.95	
Eutectic ternary carbonate salt	1.32	Mg nano particle	f=0.2, 0.5, 1, 2 wt%	1.59 to 1.93	[36]
Expanded perlite /paraffin	0.05/0.22	CNT	f=0.3, 0.5, 1 wt%, diameter=6-9 nm, length=5 µm	0.19, 0.24, 0.32	[44]
Paraffin wax	0.1264	NG	f=1, 4, 7, 10 wt%	0.3650, 0.4971, 0.5685, 0.9362	[45]
Adipic acid (48 wt%) /Sebaci acid(52 wt%)		GNP	f=0.1, 0.3, 0.5 wt%, thickness of 5-8 nm, surface area is 120-150 m2/g and particle size is 5 µm.	0.117, 0.122,0.131	[46]
paraffin/ diatomite / CNT		CNT	f=0.26 wt%, diameter is 10-20 nm and length is 5-15 µm	With CNT=1.75, without CNT=1.2	[47]
Palmitic acid	0.28	NDG	f=1, 2, 3, 4, 5 wt%,	0.34, 0.46, 0.98, 1.54, 1.73	[32]
Beeswax	0.25	GNP	<2 µm, density is 2.2 g/cm^3, f=0.05, 0.1, 0.15, 0.2, 0.25, 0.3 wt%,	1.1 to 2.89	[35]
Erythritol	0.77	C25 SCF	f=10 wt%, diameter=9 µm	3.91	[48]
		C5 SCF	f=10 wt%, diameter=9 µm	2.46	
Erythritol	0.733	SG	f=17 vol%	2.89	[49]
		EG	f=15vol %	5.46	
Paraffin wax	0.25	FLG	Type A: f=0.5, 1 wt%	~10, ~15	[33]
			Type B:f=20 wt%	~45	
			Type C:f=20 wt%	~45	
PEG/BN (BN=30 wt%)		GO	4 wt%	With GO=3 Without GO=2.77	[50]
PCM		EG	f= 25 and 35 wt%, ρ_{CPCM}=300kg/m^3	~4 , 6	[51]
			f= 25 and 35 wt%, ρ_{CPCM}=500kg/m^3	~6.5, ~8.5	
			f= 25 and 35 wt%, ρ_{CPCM}=700kg/m^3	~9, ~12	
			f= 25 and 35 wt%, ρ_{CPCM}=900kg/m^3	~11, ~15	
Paraffin wax		EG-50	Size=282 µm	2.10	[52]
RT42	0.369	EG	f=5, 10, 20, 24, 30 wt%	2.047, 3.88, 5.529, 7.464, 8.855	[53]
Paraffin wax	0.268	EG	f=20 wt%, size = 150 µm	7.65	[54]
D-Mannito PCM		EG	f=15 wt%, size = 500 µm, ρ_{CPCM}=1.80 g/cm^3	7.32	[55]
PCM		Multi-layer graphene nanocomposite	f=2 vol%	5. 8 to 14 W/m.K	[34]

To overcome this higher absorption Mills *et al.*, [27] compressed the EG into the density of 210 kg/m^3 and impregnated into the liquid RT 42 PCM. Because when the EG is compressed, it will become small in size and most of the pores will be sealed, actually, pores are good for thermal conductivity enhancement but higher pores are not good. In this study EG was compacted by applying a direct pressing method, EG doesn't need any binding materials because the direct pressing method interlocks the EG to get stick with each other. After compaction, EG absorbs less PCM compared to non-compaction but it absorbs the PCM uniformly. After absorption, there will be a noticeable volume expansion in EG. Further, EG impregnated PCM was dried naturally and it is compressed to the 789 kg/m^3 because density is directly proportional to thermal conductivity and it enhanced 16.6 W/m.K. This method controls the PCM leakage, compacted EG acts as a protection layer. To control 100 % leakage Tao *et al.,* [28] used porous graphite foam with the diameter of a 1-3 mm sphere ball by compressing at 1 Mpa for 6 hours. After that graphite foam was impregnated with liquid paraffin wax under 10 KPa for 4 hours to attain a high impregnation range, further adhesives materials were applied on the surface of graphite foam to avoid the leakages. This method blocks the leakages permanently but it restricts the thermal conduction because adhesive thermal conductivity is low however this technique enhanced a maximum of 4.98 W/m.K for 0.95 g/cm^3 and some other techniques of non-metal based composites are listed in Table 2.

IV. cPCM BASED T_{PV} REDUCTION

Maiti *et al.,* [56] performed V-through concentrated PV indoor and outdoor experiment using paraffin wax embedded with metal scrap to enhance the thermal conductivity of the PCM andthe experimental setup is shown in Fig. 6. Using metal scrap T_{PV} is regulated for a maximum of 4 hours beyond that T_{PV} started to increase but still it under control than PV without PCM. Thermal distribution occurs better than thermal distribution fin but it minimizes the total storage capacity of the PCM due to the higher volume occupancy of the metal scrap. Reportedly V-through concentrates the solar irradiance which leads to an increase in the T_{PV} abruptly compared non-concentrated PV module.

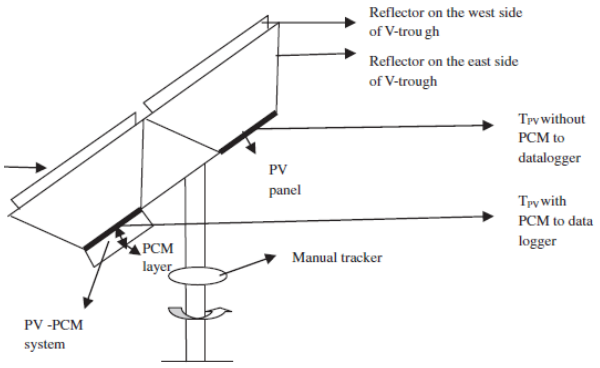

Fig. 6. V-through concentrated PV with metal scrap embedded PCM and PV without PCM [56].

Other than metal scrap, copper and graphite mixed PCM enable high thermal distribution inside the PCM and the experimental setup is shown in Fig. 7. Reportedly T_{PV} without PCM reached an average of 59℃, T_{PV} with pure PCM enables 3℃ reduction because thermal conduction resistance blocks to reduce the higher T_{PV}. The same with copper and graphite-based PCM enables 6℃ reduction as compared to PV without PCM. Copper powder enhances the thermal distribution with the help of its high thermal conductivity, the only drawback in this system is copper powder can be settled on the bottom of the PCM container will settle down.

However still this copper and graphite combination is better solution than thermal distribution fin and metal scrap because when liquid PCM starts to circulate, settled copper powder can be mixed with PCM easily but it can occur during summer or when the PCM attains high temperature [57].

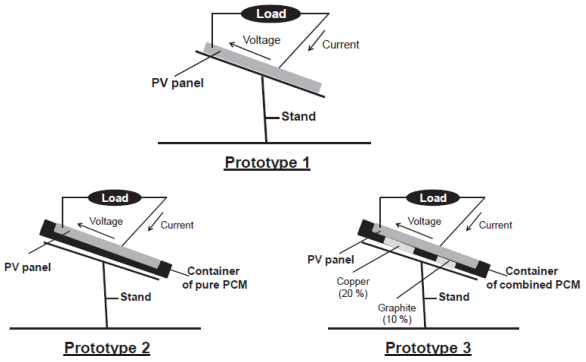

Fig. 7. Schematic diagram of PV without PCM, PV with pPCM and PV with copper and graphite combined PCM [57].

A. Selection of thermal conductivity enhancement technique

It was observed from the existing literature; metal foam is the best in terms of thermal conductivity enhancement but practical it is quite complicated to implement with the PV module. Because it will increase the total weight of the system and it is difficult in manufacturing as well. On the other hand, non-metal based additives gained high attention especially graphene-based composite PCM, but economically it is not viable for T_{PV} reduction, system cost may go higher than the T_{PV} loss. Nano PCM and other methods were enhanced less thermal conductivity than EG. So in this work, EG is selected as a thermal additive to enhance the PCM thermal conductivity.

V. PREPARATION OF EG BASED COMPOSITE PCM

A. Furnace treatment

Expandable Graphite is purchased from Metachem Manufacturing Company Pvt. Ltd, India and without further processing material placed in a furnace for volume expansion as shown in Fig. 8. This EG actual density is 0.65 g/cm^3 before volume expansion.

To expand the volume, the furnace is maintained at 500℃ for 90 seconds which leads to expanding the volume of about 300 times. After expanding, graphite

flakes will look like a worm and it is easy to spread uniformly over the entire volume of the PCM due to its higher volume with less weight. In many cases, mixing EG into PCM directly without any further compaction of EG also leads to an increasein thermal conductivity but not higher than compressed EG porous foam. Once theexpandable graphite is treated at 500℃, it expands the volume abruptly by creating high porosity. The main parameters considered in enhancing the thermal conductivity of PCM by using EG, it is necessary to compact the EG to get the desired porosity range for the required amount ofPCM impregnation unless it absorbs more PCM due to its high porosity.

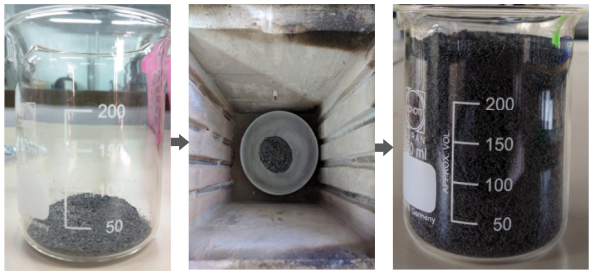

Pure EG EG before expansion EG after expansion

Fig. 8. Furnace treatment for EG expansion.

B. EG porous foam

Expanded graphite is compacted into 0.29 g/cm^3 without using an adhesive material and considering the 80 wt % of PCM which helps to increase the thermal conductivity of cPCM as well as without losing much thermal property of PCM as shown in Fig. 9. Compacted graphite porous foam is pressed to seal the unwanted pores to control the high PCM impregnation. In general, impregnating high PCM will lead to maintaining high energy capacity. But inthissituation, EG is considered as thermal additivesso it is necessary to use the optimal level of 20 wt %.

Fig. 9. Compacted EG porous foam.

C. PCM impregnation

Compacted EG porous foam is impregnated into the liquid PCM to absorb the PCM. The density of EG porous foam is nearly 3 times lower than the pPCM which leads to floating the EG porous foam during impregnation as shown in Fig. 10.

Fig. 10. EG impregnation with liquid PCM at 70℃.

Considering this floating, EG is maintained in liquid PCM for 5 hours to absorb the PCM effectively. Every ten minutes, EG porous foam is weighed until it reaches the 80 wt % PCM impregnation. However, the impregnation factor cannot reach 100 %. During compaction of EG porous foam, there will be some pores closed.

D. Thermal conductivity measurement

Composite PCM is undergone for transient plane source technique (TPS) to measure the thermal conductivityas shown in Fig. 11. Without any compaction, PCM impregnated EG porous foam bulk density reached 0.5884 g/cm^3 which is lower than pPCM density. In such cases, it is necessary to compact the cPCM. Further,cPCMis compacted intothree different densities as listed in Table 3. Increase in bulk density, K_{cPCM} increased linearly. But increasing beyond the pPCM density will lead to an increase in the thermal conductivity [51] but practically it is not suitable in the real-time experiment because leakage may occur during phase change.

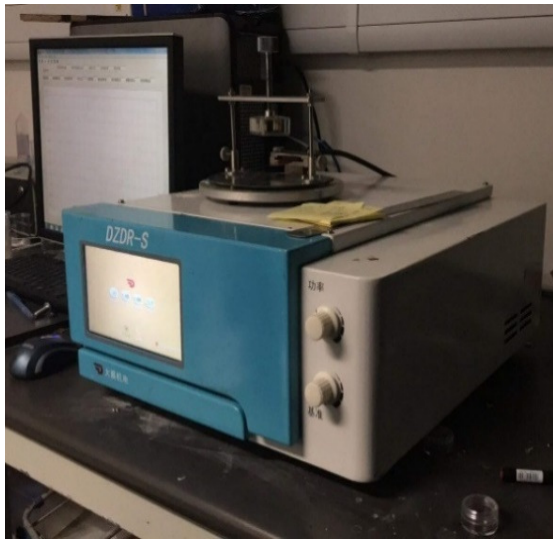

Fig. 11. Transient plane source technology (DZDR-S).

Table 3: Different bulk density of cPCM with its corresponding thermal conductivity.

Bulk density (g/cm^3)	cPCM thermal conductivity (W/m.K)
0.5884	3.9718
0.6289	4.7028
0.7928	5.6890

VI. CONCLUSION

Many existing methods show that enhancing the thermal conductivity of PCM is highly possible. Especially, graphene leads to increase higher thermal conductivity than other materials, but economically graphene composition is not viable for T_{PV} reduction, because in this case reducing T_{PV} is only to increase the performance of PV module which is suffering from the temperature loss, so economic viability is mandatory to notice. Secondly, Al and Cu metal foam enhanced high thermal conductivity, the only action to take care of in this technique is the total weight of the system because in many cases reducing T_{PV} will be an external system to reduce the T_{PV} of an already existing PV system. But where there is no restriction in the weight of the external system, their metal foam will play a major role in T_{PV} reduction, especially in small scale systems. Other than graphene and metal foam, EG gains more attention on thermal conductivity enhancement, cost and weight wise EG is favorable to install with the PV module. In this experiment, EG is considered as a thermal additive, and it is prepared into three different densities of EG impregnated PCM (cPCM) to find the thermal conductivity relationship to their corresponding density. Resulting shows that 0.7928 g/cm^3 enhanced a maximum of 5.6890 W/m.K.

VII. FUTURE SCOPE

Enhancing PCM thermal conductivity leads to minimizing the cost and total quantity of PCM in the existing thermal energy storage system as well as it increases the fast charging and discharging.

ACKNOWLEDGEMENT

Authors would like to thanks Mr. Vaithinathan Karthikeyan from the Department of Materials Science and Engineering, City University of Hong Kong for providing thermal conductivity (hot wire measurement) analyzer measurement.

Conflict of Interest. This research contains no conflict in funding, collaboration, and publication.

NOMENCLATURE

mactual	actual mass, kg
mideal	ideal mass, kg
K foam	foam thermal conductivity, W/m.K
Kf	fluid thermal conductivity, W/m.K
Vt	total volume, m^3
α	impregnation ratio, %
ρPCM	PCM density, kg/m^3
Δmi	absolute error of PCM impregnation, %
d	ligament radius
e	nodel length
εb	bulk porosity
RA, RB, RC, RD	unit cell subsection simplification quantity, mK/W

REFERENCES

[1]. Min, H. S., Fertahi, S. D., Bouhal, T. Naa, N. S. & Munaaim, M. A. C. (2019). Solar Energy development: Case study in Malaysia and Morocco. *International Journal on Emerging Technologies*, *10*(1), 106-113.

[2]. Sreenath, S., Sudhakar, K., & Yusop, A. F. (2019). SWOT Analysis of Solar PV Systems in Airport Environment. *International Journal on Emerging Technologies, 10*(2), 1-07.

[3]. Velmurugan, K. & Sukchai, S. (2019). Development of Thermal Storage System Combined with Paraffin Pre-Heating Unit for Industrial Applications. *Journal of Advanced Research in Dynamical and Control Systems*, 2019. *11*, 1456-1463.

[4]. Velmurugan, K. & Sukchai, S. (2019). Thermal Investigation of Paraffin Wax for Low-Temperature Application. *Journal of Advanced Research in Dynamical and Control Systems*, *11*, 1437-1443.

[5]. Karthikeyan, V., Sirisamphanwong, C., & Sukchai, S. (2018). Investigation on Thermal Absorptivity of PCM Matrix Material for Photovoltaic Module Temperature Reduction. In *Key Engineering Materials, 777*, 97-101. Trans Tech Publications.

[6]. Mahamudul, H., Rahman, M., Metselaar, H. S. C., Mekhilef, S., Shezan, S. A., Sohel, R., ... & Badiuzaman, W. N. I. (2016). Temperature regulation of photovoltaic module using phase change material: a numerical analysis and experimental investigation. *International journal of Photoenergy*, 1-8.

[7]. Mahamudul, H., Silakhori, M., Metselaar, I. H., Ahmad, S., & Mekhilef, S. (2014). Development of a temperature regulated photovoltaic module using phase change material for Malaysian weather condition. *the journal Optoelectronics and Advanced Materials-Rapid Communications*, *8*, 1243-1245.

[8]. Khanna, S., Reddy, K. S., & Mallick, T. K. (2018). Optimization of solar photovoltaic system integrated with phase change material. *Solar Energy*, *163*, 591-599.

[9]. Waqas, A., & Jie, J. (2018). Effectiveness of Phase Change Material for Cooling of Photovoltaic Panel for Hot Climate. *Journal of Solar Energy Engineering*, *140*(4), 041006. (Page No.)

[10]. Biwole, P. H., Eclache, P., & Kuznik, F. (2013). Phase-change materials to improve solar panel's performance. *Energy and Buildings*, *62*, 59-67.

[11]. Huang, M. J., Eames, P. C. & Norton, B. (2004). Thermal regulation of building-integrated photovoltaics using phase change materials. *International Journal of Heat and Mass Transfer*, *47*(12), 2715-2733.

[12]. Biwole, P., Eclache, P., & Kuznik, F. (2011). Improving the performance of solar panels by the use of phase-change materials. In *World Renewable Energy Congress-Sweden; 8-13 May; 2011; Linköping; Sweden*,*57*,2953-2960). Linköping University Electronic Press.

[13]. Nehari, T., Benlakam, M., & Nehari, D. (2016). Effect of the Fins Length for the Passive Cooling of the Photovoltaic Panels. *Periodica Polytechnica Mechanical Engineering*, *60*(2), 89-95.

[14]. Khanna, S., Reddy, K. S., & Mallick, T. K. (2018). Optimization of finned solar photovoltaic phase change material (finned pv pcm) system. *International Journal of Thermal Sciences*, *130*, 313-322.
[15]. Huang, M. J., Eames, P. C., & Norton, B. (2006). Phase change materials for limiting temperature rise in building integrated photovoltaics. *Solar Energy*, *80*(9), 1121-1130.
[16]. Sheet, M.d., RS Components Ltd. United Kingdom, 2000.
[17]. Nehari, T., Benlekkam, M., Nehari, D., & Youcefi, A. (2016). The Effect of Inclination on the Passive cooling of the solar PV panel by using Phase change Material. *International Journal of Renewable Energy Research (IJRER)*, *6*(1), 132-139.
[18]. Xiao, X., Zhang, P., & Li, M. (2013). Preparation and thermal characterization of paraffin/metal foam composite phase change material. *Applied energy*, *112*, 1357-1366.
[19]. Augusta, A., Reiterb, A., Kneerb, A., Selzera, M., & Nestlera, B. (2018). Effective Thermal Conductivity of Composite Materials Based on Open Cell Foams. *stainless steel*, *2*(1), 33-45.
[20]. Xiao, X., Zhang, P., & Li, M. (2014). Effective thermal conductivity of open-cell metal foams impregnated with pure paraffin for latent heat storage. *International Journal of Thermal Sciences*, *81*, 94-105.
[21]. Wang, G., Wei, G., Xu, C., Ju, X., Yang, Y., & Du, X. (2019). Numerical simulation of effective thermal conductivity and pore-scale melting process of PCMs in foam metals. *Applied Thermal Engineering*, *147*, 464-472.
[22]. Sutanto, B., & Indartono, Y. S. (2019). Computational fluid dynamic (CFD) modelling of floating photovoltaic cooling system with loop thermosiphon. In *AIP Conference Proceedings*, *2062*(1), pp. 020011). AIP Publishing.
[23]. Boomsma, K., & Poulikakos, D. (2001). On the effective thermal conductivity of a three-dimensionally structured fluid-saturated metal foam. *International Journal of Heat and Mass Transfer*, *44*(4), 827-836.
[24]. Di Giorgio, P., Iasiello, M., Viglione, A., Mameli, M., Filippeschi, S., Di Marco, P., ... & Bianco, N. (2017, January). Numerical analysis of a paraffin/metal foam Composite for Thermal Storage. In *Journal of Physics: Conference Series*, *796*(1), p. 012032. IOP Publishing.
[25]. Du, Y., & Ding, Y. (2016). Towards improving charge/discharge rate of latent heat thermal energy storage (LHTES) by embedding metal foams in phase change materials (PCMs). *Chemical Engineering and Processing: Process Intensification*, *108*, 181-188.
[26]. Huang, X., Lin, Y., Alva, G., & Fang, G. (2017). Thermal properties and thermal conductivity enhancement of composite phase change materials using myristyl alcohol/metal foam for solar thermal storage. *Solar Energy Materials and Solar Cells*, *170*, 68-76.
[27]. Mills, A., Farid, M., Selman, J. R., & Al-Hallaj, S. (2006). Thermal conductivity enhancement of phase change materials using a graphite matrix. *Applied Thermal Engineering*, *26*(14-15), 1652-1661.
[28]. Tao, Z., Wang, H., Liu, J., Zhao, W., Liu, Z., & Guo, Q. (2017). Dual-level packaged phase change materials–thermal conductivity and mechanical properties. *Solar Energy Materials and Solar Cells*, *169*, 222-225.
[29]. Wang, C., Lin, T., Li, N., & Zheng, H. (2016). Heat transfer enhancement of phase change composite material: Copper foam/paraffin. *Renewable Energy*, *96*, 960-965.
[30]. Li, T. X., Wu, D. L., He, F., & Wang, R. Z. (2017). Experimental investigation on copper foam/hydrated salt composite phase change material for thermal energy storage. *International Journal of Heat and Mass Transfer*, *115*, 148-157.
[31]. Abdulmunem, A. R. (2017). Passive cooling by utilizing thecombined pcm/aluminum foam matrix to improve solar panels performance: indoor investigation. *Iraqi journal of mechanical and material engineering*, *17*(4), 712-723.
[32]. Mehrali, M., Latibari, S. T., Mehrali, M., Mahlia, T. M. I., Sadeghinezhad, E., & Metselaar, H. S. C. (2014). Preparation of nitrogen-doped graphene/palmitic acid shape stabilized composite phase change material with remarkable thermal properties for thermal energy storage. *Applied energy*, *135*, 339-349.
[33]. Goli, P., Legedza, S., Dhar, A., Salgado, R., Renteria, J., & Balandin, A. A. (2014). Graphene-enhanced hybrid phase change materials for thermal management of Li-ion batteries. *Journal of Power Sources*, *248*, 37-43.
[34]. Shahil, K. M., & Balandin, A. A. (2012). Graphene–multilayer graphene nanocomposites as highly efficient thermal interface materials. *Nano letters*, *12*(2), 861-867.
[35]. Amin, M., Putra, N., Kosasih, E. A., Prawiro, E., Luanto, R. A., & Mahlia, T. M. I. (2017). Thermal properties of beeswax/graphene phase change material as energy storage for building applications. *Applied Thermal Engineering*, *112*, 273-280.
[36]. Tian, H., Du, L., Wei, X., Deng, S., Wang, W., & Ding, J. (2017). Enhanced thermal conductivity of ternary carbonate salt phase change material with Mg particles for solar thermal energy storage. *Applied Energy*, *204*, 525-530.
[37]. Ji, H., Sellan, D. P., Pettes, M. T., Kong, X., Ji, J., Shi, L., & Ruoff, R. S. (2014). Enhanced thermal conductivity of phase change materials with ultrathin-graphite foams for thermal energy storage. *Energy & Environmental Science*, *7*(3), 1185-1192.
[38]. Kim, S., & Drzal, L. T. (2009). High latent heat storage and high thermal conductive phase change materials using exfoliated graphite nanoplatelets. *Solar Energy Materials and Solar Cells*, *93*(1), 136-142.
[39]. Fan, L. W., Fang, X., Wang, X., Zeng, Y., Xiao, Y. Q., Yu, Z. T., ... & Cen, K. F. (2013). Effects of various carbon nanofillers on the thermal conductivity and energy storage properties of paraffin-based nanocomposite phase change materials. *Applied Energy*, *110*, 163-172.
[40]. Nomura, T., Tabuchi, K., Zhu, C., Sheng, N., Wang, S., & Akiyama, T. (2015). High thermal conductivity phase change composite with percolating carbon fiber network. *Applied energy*, *154*, 678-685.
[41]. Sarı, A., & Karaipekli, A. (2007). Thermal conductivity and latent heat thermal energy storage characteristics of paraffin/expanded graphite composite

as phase change material. *Applied Thermal Engineering*, *27*(8-9), 1271-1277.
[42]. Sarı, A., & Karaipekli, A. (2009). Preparation, thermal properties and thermal reliability of palmitic acid/expanded graphite composite as form-stable PCM for thermal energy storage. *Solar Energy Materials and Solar Cells*, *93*(5), 571-576.
[43]. Karaipekli, A., Sarı, A., & Kaygusuz, K. (2007). Thermal conductivity improvement of stearic acid using expanded graphite and carbon fiber for energy storage applications. *Renewable Energy*, *32*(13), 2201-2210.
[44]. Karaipekli, A., Biçer, A., Sarı, A., & Tyagi, V. V. (2017). Thermal characteristics of expanded perlite/paraffin composite phase change material with enhanced thermal conductivity using carbon nanotubes. *Energy conversion and management*, *134*, 373-381.
[45]. Li, M. (2013). A nano-graphite/paraffin phase change material with high thermal conductivity. *Applied energy*, *106*, 25-30.
[46]. Seki, Y., İnce, Ş., Ezan, M. A., Turgut, A., & Erek, A. (2015). Graphite nanoplates loading into eutectic mixture of Adipic acid and Sebacic acid as phase change material. *Solar Energy Materials and Solar Cells*, *140*, 457-463.
[47]. Xu, B., & Li, Z. (2014). Paraffin/diatomite/multi-wall carbon nanotubes composite phase change material tailor-made for thermal energy storage cement-based composites. *Energy*, *72*, 371-380.
[48]. Zhang, Q., Luo, Z., Guo, Q., & Wu, G. (2017). Preparation and thermal properties of short carbon fibers/erythritol phase change materials. *Energy conversion and management*, *136*, 220-228.
[49]. Oya, T., Nomura, T., Tsubota, M., Okinaka, N., & Akiyama, T. (2013). Thermal conductivity enhancement of erythritol as PCM by using graphite and nickel particles. *Applied Thermal Engineering*, *61*(2), 825-828.
[50]. Yang, J., Tang, L. S., Bao, R. Y., Bai, L., Liu, Z. Y., Xie, B. H., ... & Yang, W. (2018). Hybrid network structure of boron nitride and graphene oxide in shape-stabilized composite phase change materials with enhanced thermal conductivity and light-to-electric energy conversion capability. *Solar Energy Materials and Solar Cells*, *174*, 56-64.
[51]. Ling, Z., Chen, J., Xu, T., Fang, X., Gao, X., & Zhang, Z. (2015). Thermal conductivity of an organic phase change material/expanded graphite composite across the phase change temperature range and a novel thermal conductivity model. *Energy conversion and management*, *102*, 202-208.
[52]. Cheng, W. L., Li, W. W., Nian, Y. L., & Xia, W. D. (2018). Study of thermal conductive enhancement mechanism and selection criteria of carbon-additive for composite phase change materials. *International Journal of Heat and Mass Transfer*, *116*, 507-511.
[53]. Wang, T., Wang, S., & Wu, W. (2017). Experimental study on effective thermal conductivity of microcapsules based phase change composites. *International Journal of Heat and Mass Transfer*, *109*, 930-937.
[54]. Wu, W., Zhang, G., Ke, X., Yang, X., Wang, Z., & Liu, C. (2015). Preparation and thermal conductivity enhancement of composite phase change materials for electronic thermal management. *Energy conversion and management*, *101*, 278-284.
[55]. Xu, T., Chen, Q., Huang, G., Zhang, Z., Gao, X., & Lu, S. (2016). Preparation and thermal energy storage properties of d-Mannitol/expanded graphite composite phase change material. *Solar Energy Materials and Solar Cells*, *155*, 141-146.
[56]. Maiti, S., Banerjee, S., Vyas, K., Patel, P., & Ghosh, P. K. (2011). Self regulation of photovoltaic module temperature in V-trough using a metal–wax composite phase change matrix. *Solar energy*, *85*(9), 1805-1816.
[57]. Hachem, F., Abdulhay, B., Ramadan, M., El Hage, H., El Rab, M. G., & Khaled, M. (2017). Improving the performance of photovoltaic cells using pure and combined phase change materials–Experiments and transient energy balance. *Renewable energy*, *107*, 567-575.

How to cite this article: Karthikeyan, V., Prasannaa, P., Sathishkumar, N., Emsaeng, Kanchanok, Sukchai, Sukruedee and Sirisamphanwong, Chatchai (2019). Selection and Preparation of Suitable Composite Phase Change Material for PV Module Cooling. *International Journal on Emerging Technologies*, *10*(4): 385–394.